

SATELLITE ATTITUDE TRACKING BY QUATERNION-BASED BACKSTEPPING

Raymond Kristiansen ^{*,1} Per Johan Nicklasson ^{*,2}
Jan Tommy Gravdahl ^{**3}

** Department of Space Technology
Narvik University College, Norway*

*** Department of Engineering Cybernetics
Norwegian University of Science and Technology, Norway*

Abstract: In this paper a result on attitude tracking control of a micro satellite by integrator backstepping based on quaternion feedback is presented, and the controller is shown to render the system equilibrium point UGAS by application of the LaSalle-Yoshizawa theorem. This is a part of a study of possible control methods for the spacecraft ESEO, a spacecraft included in the SSETI project initiated by ESA. ESEO is actuated by four reaction control thrusters and one reaction wheel, and simulation results based on data from the satellite are presented. *Copyright © 2005 IFAC*

Keywords: Satellite control, attitude tracking, quaternion feedback, integrator backstepping.

1. INTRODUCTION

1.1 Background

The European Space Agency (ESA) has initiated a project named Student Space Exploration & Technology Initiative (SSETI), a project where students from twelve European countries are collaborating in building the European Student Earth Orbiter (ESEO). Based on this project, we have started an investigation of possible control methods. ESEO is designed to be $60 \times 60 \times 80$ cm³, and its weight should not exceed 120 kg. For attitude and orbit control, the ESEO will use one reaction wheel for control of the pitch movement, four thrusters for attitude control (ACS thrusters), one main orbit control thruster (OCS thruster) for orbital maneuvers, and additional four reaction control thrusters (RCS thrusters) used to correct orbital maneuvers since the OCS thrust vector

might not go through the center of mass. The RCS thrusters are also used as a redundancy for the ACS thrusters. The ESEO will take pictures of both the earth and the moon, in addition to performing several attitude maneuvers to test and qualify the attitude control and determination system. Several linear and nonlinear attitude control approaches for the ESEO has been proposed in (Antonsen, 2004) and (Topland and Gravdahl, 2004). The next mission planned for the SSETI project is the European Student Moon Orbiter (ESMO), which is proposed to be built similar to ESEO. For more information about the SSETI project, see <http://www.sseti.net>.

1.2 Contribution

The possibility to perform attitude tracking by a satellite serves important purposes for spacecraft missions. For satellites with limited supply of electric power, and especially those depending on electric propulsion for attitude and orbit control, the possibility of tracking a sun-optimal trajectory can be vital for long-life

¹ PhD Student, rayk@hin.no

² Associate Professor, pjn@hin.no

³ Associate Professor, tommy.gravdahl@itk.ntnu.no

missions. Some satellites must have the possibility for attitude tracking to be able to complete the objectives of the mission, for instance satellites sent out to take pictures or collect measurements from objects far away, or maintain high precision pointing towards object on the ground, as proposed in (Romano and Agrawal, 2003). Also, increasing demands on the use of satellites as communication nodes makes it necessary for satellites to track other satellites passing by, with a high degree of accuracy, with intention of transmitting or receiving data.

In this article we propose a quaternion-based integrator backstepping approach for tracking a desired rotation path for the ESEO, with use of the ACS thrusters and a reaction wheel. A somewhat similar approach to attitude tracking by means of magnetorquers only has been proposed in (Wang *et al.*, 1998), where a backstepper is used for attitude control in conjunction with a sliding mode controller for tracking of the desired angular velocity. Also, a similar controller has been derived in (Wen and Kreutz-Delgado, 1991) as a feedback linearizing controller with constant feedback gains. Attitude tracking of rigid bodies without use of angular velocity feedback has been proposed in (Akella, 2001) and more generally in (Caccavale and Villani, 1999). The concept of integrator backstepping was according to (Fossen, 2002) introduced in the late eighties. Quaternion feedback control based on Lyapunov stability theory, the wider group in which integrator backstepping adheres to, was proposed in (Fjellstad, 1994) for regulation of underwater vehicles, and its application to spacecraft rotation was examined in (Joshi *et al.*, 1995), and later in (Jensen and Wisniewski, 2001).

The advantage of a four-parameter attitude representation such as quaternions as opposed to more conventional three-parameter representations as the Euler angle conventions, is the avoidance of singular points in the representation, together with better numerical properties (Egeland and Gravdahl, 2002). However, the use of redundant parameters to avoid singularities also includes a redundancy of the mathematical representations for a given physical attitude. Therefore, a given physical attitude for a rigid body will have two mathematical representation, where one of these includes a rotation of $\pm 2\pi$ about an axis. For equilibrium points, care must be taken to avoid that one of the mathematical representations of a given attitude is left unstable, causing an unwanted or less optimal rotation of the satellite to the desired attitude.

The rest of the paper is organized as follows: Section 2 defines the different reference frames used and reviews the mathematical models of rigid-body dynamics and kinematics. The controller design is performed in section 3, and simulation results of the ESEO with the derived controller is presented in section 4. Conclusions and possibilities of future work comprises section 5.

2. MODELING

2.1 Coordinate frames

The different reference frames used throughout the paper are given as follows:

Earth-Centered Inertial (ECI) Reference Frame

This frame is denoted \mathcal{F}_i , and has its origin located in the center of the earth. Its z -axis is directed along the rotation axis of the earth towards the celestial north pole, the x -axis is directed towards the vernal equinox, and finally the direction of the y -axis completes a right handed orthogonal frame.

Orbit Reference Frame

The orbit frame, denoted \mathcal{F}_o , has its origin located in the mass center of the satellite. The z -axis is pointing towards the center of the earth, and the x -axis is directed forward in the travelling direction of the satellite, tangentially to the orbit. Assuming a near circular orbit, the orbit frame rotate relative to the ECI frame with an angular velocity of approximately

$$\omega_o \approx \sqrt{\frac{\mu_g}{r_c^3}} \quad (1)$$

where μ_g is the Earth's gravitational coefficient and r_c is the distance from the frame origin to the center of the earth. Satellite rotation about the x -, y - and z -axis is named roll, pitch and yaw respectively, which constitute the attitude of the satellite.

Body Reference Frame This frame has, similar to the orbit frame, its origin located in the satellite center of mass, but its axes are locked to the satellite and coincide with the principal axis of inertia. The frame is denoted \mathcal{F}_b .

Desired Reference Frame This is a rotating frame that describe the desired rotation of the satellite, and is denoted \mathcal{F}_d .

2.2 Kinematics

Rotation between the previously described reference frames is done by rotation matrices, members of the special orthogonal group of order three, i.e.

$$SO(3) = \{\mathbf{R} | \mathbf{R} \in \mathbb{R}^{3 \times 3}, \mathbf{R}^T \mathbf{R} = \mathbf{I}, \det \mathbf{R} = 1\}$$

where \mathbf{I} is the 3×3 identity matrix. A rotation matrix for a rotation θ about an arbitrary unit vector \mathbf{k} can be angle-axis parameterized as

$$\mathbf{R}_{k,\theta} = \mathbf{I} + \mathbf{S}(\mathbf{k}) \sin \theta + \mathbf{S}^2(\mathbf{k}) (1 - \cos \theta) \quad (2)$$

and rotation of a vector \mathbf{r} from frame a to frame b is written as $\mathbf{r}^b = \mathbf{R}_a^b \mathbf{r}^a$. In general, the rotation matrix describing rotations from the orbit frame to the body frame can be described by

$$\mathbf{R}_o^b = (\mathbf{c}_1 \ \mathbf{c}_2 \ \mathbf{c}_3) \quad (3)$$

where the elements c_i are the directional cosines. The time derivative of a matrix \mathbf{R}_a^b can according to (Egeland and Gravdahl, 2002) be expressed as

$$\dot{\mathbf{R}}_a^b = \mathbf{S}(\boldsymbol{\omega}_{ab}^a) \mathbf{R}_a^b = \mathbf{R}_a^b \mathbf{S}(\boldsymbol{\omega}_{ab}^b) \quad (4)$$

where $\boldsymbol{\omega}_{ab}^b$ is the angular velocity of frame b relative to frame a represented in frame b and $\mathbf{S}(\cdot)$ is the cross product operator given by

$$\mathbf{S}(\boldsymbol{\omega}) = \boldsymbol{\omega} \times = \begin{pmatrix} 0 & -\omega_z & \omega_y \\ \omega_z & 0 & -\omega_x \\ -\omega_y & \omega_x & 0 \end{pmatrix}, \quad \boldsymbol{\omega} = \begin{pmatrix} \omega_x \\ \omega_y \\ \omega_z \end{pmatrix}$$

Similar to (4), the time derivative of the directional cosines in (3) can be expressed as

$$\dot{c}_i = \mathbf{S}(c_i) \boldsymbol{\omega}_{ob}^b$$

The rotation matrix in (2) can be expressed by an Euler parameter representation given as

$$\mathbf{R}_{\eta, \boldsymbol{\epsilon}} = \mathbf{I} + 2\eta \mathbf{S}(\boldsymbol{\epsilon}) + 2\mathbf{S}^2(\boldsymbol{\epsilon}) \quad (5)$$

where

$$\eta = \cos(\theta/2) \in \mathbb{R} \quad (6)$$

$$\boldsymbol{\epsilon} = \mathbf{k} \sin(\theta/2) \in \mathbb{R}^3 \quad (7)$$

are the Euler parameters, which satisfies the constraint

$$\eta^2 + \boldsymbol{\epsilon}^T \boldsymbol{\epsilon} = 1 \quad (8)$$

A vector consisting of the Euler parameters

$$\mathbf{q} = [\eta \ \boldsymbol{\epsilon}^T]^T$$

is in the following treated as a unit quaternion vector, and referred to as a quaternion. The inverse rotation is given by the complex conjugate of \mathbf{q} as

$$\bar{\mathbf{q}} = [\eta \ -\boldsymbol{\epsilon}^T]^T$$

It should be noted that if \mathbf{q} represents a given attitude, then $-\mathbf{q}$ represents the same attitude after a rotation of $\pm 2\pi$ about an arbitrary axis. Hence, even though $\mathbf{q} \neq -\mathbf{q}$ mathematically, they represent the same physical attitude.

The kinematic differential equations can be found from (4) together with (6)-(7) as

$$\dot{\eta} = -\frac{1}{2} \boldsymbol{\epsilon}^T \boldsymbol{\omega}_{ob}^b \quad (9)$$

$$\dot{\boldsymbol{\epsilon}} = \frac{1}{2} [\eta \mathbf{I} + \mathbf{S}(\boldsymbol{\epsilon})] \boldsymbol{\omega}_{ob}^b \quad (10)$$

The deviation between the current attitude $\mathbf{q} = [\eta \ \boldsymbol{\epsilon}]^T$ and the desired attitude $\mathbf{q}_d = [\eta_d \ \boldsymbol{\epsilon}_d]^T$ is given by the quaternion product (Egeland and Gravdahl, 2002) as

$$\begin{bmatrix} \tilde{\eta} \\ \tilde{\boldsymbol{\epsilon}} \end{bmatrix} = \begin{bmatrix} \eta_d \\ \boldsymbol{\epsilon}_d \end{bmatrix} \otimes \begin{bmatrix} \eta \\ -\boldsymbol{\epsilon} \end{bmatrix} \quad (11)$$

$$= \begin{bmatrix} \eta_d \eta + \boldsymbol{\epsilon}_d^T \boldsymbol{\epsilon} \\ \eta_d \boldsymbol{\epsilon} - \eta \boldsymbol{\epsilon}_d - \mathbf{S}(\boldsymbol{\epsilon}_d) \boldsymbol{\epsilon} \end{bmatrix} \quad (12)$$

and the error dynamics can according to (Fjellstad, 1994) be expressed as

$$\dot{\tilde{\eta}} = -\frac{1}{2} \tilde{\boldsymbol{\epsilon}}^T \tilde{\boldsymbol{\omega}} \quad (13)$$

$$\dot{\tilde{\boldsymbol{\epsilon}}} = \frac{1}{2} [\tilde{\eta} \mathbf{I} + \mathbf{S}(\tilde{\boldsymbol{\epsilon}})] \tilde{\boldsymbol{\omega}} \quad (14)$$

where

$$\tilde{\boldsymbol{\omega}} = \boldsymbol{\omega}_{db}^b = \boldsymbol{\omega}_{ib}^b - \boldsymbol{\omega}_{id}^b \quad (15)$$

is the angular velocity error between the body reference frame and the desired reference frame.

2.3 Dynamics

With the assumptions of rigid body movement, the dynamical model of a satellite can be found from Euler's moment equation as (Sidi, 1997)

$$\mathbf{J} \dot{\boldsymbol{\omega}}_{ib}^b = -\boldsymbol{\omega}_{ib}^b \times (\mathbf{J} \boldsymbol{\omega}_{ib}^b) + \boldsymbol{\tau}_d^b + \boldsymbol{\tau}_a^b \quad (16)$$

$$\boldsymbol{\omega}_{ob}^b = \boldsymbol{\omega}_{ib}^b + \omega_o \mathbf{c}_2 \quad (17)$$

where \mathbf{J} is the satellite inertia matrix, $\boldsymbol{\omega}_{ib}^b$ is the angular velocity of the satellite body frame relative to the inertial frame and $\boldsymbol{\omega}_{ob}^b$ is the angular velocity of the satellite body frame relative to the orbit frame, all expressed in the body frame. The parameter $\boldsymbol{\tau}_d^b$ is the total disturbance torque, $\boldsymbol{\tau}_a^b$ is the actuator torque, and \mathbf{c}_2 is the directional cosine vector from (3). With (15) the angular velocity error dynamics can be expressed as

$$\begin{aligned} \mathbf{J} \dot{\tilde{\boldsymbol{\omega}}} &= \mathbf{J} \dot{\boldsymbol{\omega}}_{ib}^b - \mathbf{J} \dot{\boldsymbol{\omega}}_{id}^b \\ &= -\boldsymbol{\omega}_{ib}^b \times (\mathbf{J} \boldsymbol{\omega}_{ib}^b) + \boldsymbol{\tau}_d^b + \boldsymbol{\tau}_a^b - \mathbf{J} \dot{\boldsymbol{\omega}}_{id}^b \end{aligned} \quad (18)$$

2.4 Disturbance torques

The disturbance torques influencing on a satellite in its orbit is caused by both internal and external effects. Internal disturbances owes mostly to electromagnetic torques and fuel sloshing. External disturbances are dominated by the gravity gradient torque and aerodynamic drag, but also solar radiation and wind, variations in the gravitational field and collisions with meteoroids could be mentioned. These torques differ very much in magnitude, but relative to the control torques from the satellite they are small. In accordance with the discussion performed in (Antonsen, 2004), all disturbance torques are neglected in the following, except for the gravity gradient torque, which can be expressed as

$$\boldsymbol{\tau}_g^b = 3\omega_0^2 \mathbf{c}_3 \times (\mathbf{J} \mathbf{c}_3) \quad (19)$$

2.5 Actuator torque

2.5.1. Actuator dynamics The ESEO satellite will be equipped with four reaction thrusters and one reaction wheel mounted on the y -axis of the satellite body for attitude control, and the control torque from these thrusters can according to (Antonsen, 2004) be expressed as

$$\boldsymbol{\tau}_a^b = \boldsymbol{\tau}_t^b + \boldsymbol{\tau}_w^b = \mathbf{B}_a \mathbf{u} + \mathbf{D}_a \boldsymbol{\omega}_{ib}^b \quad (20)$$

where \mathbf{u} is the vector of actuator torques given as

$$\mathbf{u} = [F_1 \ F_2 \ F_3 \ F_4 \ \dot{h}_{wy}]^T$$

where F_i is the magnitude of thrust from the i 'th thruster and h_{wy} is the angular momentum of the reaction wheel. The actuator matrix \mathbf{B}_a contains elements from the reaction wheel and thrusters torques, and the disturbance matrix \mathbf{D}_a contains dynamic terms added from the angular momentum in the reaction wheel. In particular, we have

$$\mathbf{B}_a^T = \frac{\sqrt{2}}{2} \begin{bmatrix} -r_z & r_z & -r_x + r_y \\ r_z & r_z & r_x - r_y \\ -r_z & -r_z & r_x - r_y \\ r_z & -r_z & -r_x + r_y \\ 0 & \sqrt{2} & 0 \end{bmatrix} \quad (21)$$

where r_j , $j = x, y, z$ are the components of the common thruster distance from the satellite center of mass, due to the symmetric placement of the thrusters, and

$$\mathbf{D}_a = \begin{bmatrix} 0 & 0 & -h_{wy} \\ 0 & 0 & 0 \\ h_{wy} & 0 & 0 \end{bmatrix}$$

The matrix \mathbf{B}_a in (21) is rectangular, due to the fact that the number of actuators exceeds the degrees of freedom in the control problem. To find the desired actuator input level, the Moore-Penrose pseudoinverse, as found in (Strang, 1988), is applicable. Hence, equation (20) suggests that \mathbf{u} can be computed as

$$\mathbf{u} = \mathbf{B}_a^\dagger [\boldsymbol{\tau}_a^b - \mathbf{D}_a \boldsymbol{\omega}_{ib}^b]$$

where \mathbf{B}_a^\dagger is the aforementioned pseudoinverse given as

$$\mathbf{B}_a^\dagger = \mathbf{B}_a^T (\mathbf{B}_a \mathbf{B}_a^T)^{-1}$$

which in the case of the ESEO actuator combination can be shown to satisfy

$$\mathbf{B}_a \mathbf{B}_a^\dagger = \mathbf{I}$$

2.5.2. Thruster implementation Reaction thrusters are by nature on-off devices and are normally only capable of providing fixed torque. In this paper, bang-bang control with deadzone, as given in (Song and Agrawal, 2001) is used to control the thrusters. This is a discontinuous control method that is simple in formulation and easy to implement, but can result in excessive thruster action. It is based on a saturation function, so that the thrusters are fired when the commanded torque exceeds a defined upper limit. Increasing the deadzone and the corresponding upper limit will decrease the fuel consumption, but increase the attitude error.

3. CONTROLLER DESIGN

3.1 Integrator backstepping

The controller derived in this section is inspired by (Fossen, 2002) and (Krstić *et al.*, 1995), and the goal

is an integrator backstepping control law for tracking an arbitrary smooth trajectory $\mathbf{q}_d(t) = [\eta_d \ \boldsymbol{\epsilon}_d^T]^T$.

Step 1 The first step in the integrator backstepping approach involves control of (13) and (14), and the first backstepping variable is chosen as

$$\mathbf{z}_1 = \begin{bmatrix} 1 - |\tilde{\eta}| \\ \tilde{\boldsymbol{\epsilon}} \end{bmatrix} \quad (22)$$

where $\tilde{\eta}$ and $\tilde{\boldsymbol{\epsilon}}$ are given from the quaternion product in (12). Perfect tracking of the rotation path can be expressed in quaternion notation as (Fjellstad, 1994)

$$\mathbf{q}(t) = \mathbf{q}_d(t) \quad \Leftrightarrow \quad \tilde{\mathbf{q}}(t) = \begin{bmatrix} \pm 1 \\ \mathbf{0} \end{bmatrix} \quad (23)$$

A virtual control input is defined as

$$\tilde{\boldsymbol{\omega}} = \boldsymbol{\alpha}_1 + \mathbf{z}_2 \quad (24)$$

where $\boldsymbol{\alpha}_1$ is a stabilizing function and \mathbf{z}_2 is a new state variable. This, together with (22) leaves the \mathbf{z}_1 -system as

$$\begin{aligned} \dot{\mathbf{z}}_1 &= \begin{bmatrix} -\text{sgn}(\tilde{\eta}) \dot{\tilde{\eta}} \\ \dot{\tilde{\boldsymbol{\epsilon}}} \end{bmatrix} \\ &= \frac{1}{2} \begin{bmatrix} \text{sgn}(\tilde{\eta}) \tilde{\boldsymbol{\epsilon}}^T \\ \tilde{\eta} \mathbf{I} + \mathbf{S}(\tilde{\boldsymbol{\epsilon}}) \end{bmatrix} \tilde{\boldsymbol{\omega}} \\ &= \frac{1}{2} \mathbf{G}^T(\tilde{\mathbf{q}}) (\boldsymbol{\alpha}_1 + \mathbf{z}_2) \end{aligned} \quad (25)$$

where

$$\mathbf{G}^T(\tilde{\mathbf{q}}) = \begin{bmatrix} \text{sgn}(\tilde{\eta}) \tilde{\boldsymbol{\epsilon}}^T \\ \tilde{\eta} \mathbf{I} + \mathbf{S}(\tilde{\boldsymbol{\epsilon}}) \end{bmatrix}$$

The signum function $\text{sgn}(x)$ is defined nonzero as

$$\text{sgn}(x) = \begin{cases} -1, & x < 0 \\ 1, & x \geq 0 \end{cases}$$

to avoid a singularity when $\tilde{\eta} = 0$. With some calculations, it can be shown that

$$\mathbf{G}(\tilde{\mathbf{q}}) \mathbf{z}_1 = \mathbf{0} \quad \Leftrightarrow \quad \text{sgn}(\tilde{\eta}) \tilde{\boldsymbol{\epsilon}} = \mathbf{0} \quad (26)$$

A Lyapunov Function Candidate (LFC) can now be chosen as

$$V_1 = \mathbf{z}_1^T \mathbf{z}_1 \quad (27)$$

$$\dot{V}_1 = 2\mathbf{z}_1^T \dot{\mathbf{z}}_1 = \mathbf{z}_1^T \mathbf{G}^T(\tilde{\mathbf{q}}) (\boldsymbol{\alpha}_1 + \mathbf{z}_2) \quad (28)$$

Furthermore, the stabilizing function $\boldsymbol{\alpha}_1$ is chosen as

$$\boldsymbol{\alpha}_1 = -\mathbf{K}_1 \mathbf{G}(\tilde{\mathbf{q}}) \mathbf{z}_1 \quad (29)$$

where $\mathbf{K}_1 = \mathbf{K}_1^T > 0$ is a feedback gain matrix. Inserting this result into the LFC in (28) yields

$$\dot{V}_1 = -\mathbf{z}_1^T \mathbf{G}^T \mathbf{K}_1 \mathbf{G} \mathbf{z}_1 + \mathbf{z}_1^T \mathbf{G}^T \mathbf{z}_2$$

where the argument of the matrix $\mathbf{G}(\tilde{\mathbf{q}})$ are left out for simplicity. It should be noted that $\mathbf{G}^T \mathbf{K}_1 \mathbf{G}$ is a symmetric positive semidefinite matrix. The \mathbf{z}_1 -system from (25) now turns into

$$\begin{aligned} \dot{\mathbf{z}}_1 &= \frac{1}{2} \mathbf{G}^T (\boldsymbol{\alpha}_1 + \mathbf{z}_2) \\ &= -\frac{1}{2} \mathbf{G}^T \mathbf{K}_1 \mathbf{G} \mathbf{z}_1 + \frac{1}{2} \mathbf{G}^T \mathbf{z}_2 \end{aligned}$$

Step 2 For the second step, the \mathbf{z}_2 -dynamics can be found by rewriting and differentiating (24) as

$$\dot{\mathbf{z}}_2 = \dot{\tilde{\boldsymbol{\omega}}} - \dot{\boldsymbol{\alpha}}_1$$

and insertion of (18) leaves

$$\begin{aligned} \mathbf{J}\dot{\mathbf{z}}_2 &= \mathbf{J}\dot{\tilde{\boldsymbol{\omega}}} - \mathbf{J}\dot{\boldsymbol{\alpha}}_1 \\ &= \boldsymbol{\tau}_a^b + \boldsymbol{\tau}_g^b - \boldsymbol{\omega}_{ib}^b \times (\mathbf{J}\boldsymbol{\omega}_{ib}^b) - \mathbf{J}\dot{\boldsymbol{\omega}}_{id}^b - \mathbf{J}\dot{\boldsymbol{\alpha}}_1 \end{aligned} \quad (30)$$

A second LFC can now be expressed as

$$\begin{aligned} V_2 &= V_1 + \frac{1}{2}\mathbf{z}_2^T \mathbf{J}\mathbf{z}_2 \\ \dot{V}_2 &= \dot{V}_1 + \mathbf{z}_2^T \mathbf{J}\dot{\mathbf{z}}_2 \\ &= \dot{V}_1 + \mathbf{z}_2^T [\boldsymbol{\tau}_a^b + \boldsymbol{\tau}_g^b - \boldsymbol{\omega}_{ib}^b \times (\mathbf{J}\boldsymbol{\omega}_{ib}^b) \\ &\quad - \mathbf{J}\dot{\boldsymbol{\omega}}_{id}^b - \mathbf{J}\dot{\boldsymbol{\alpha}}_1] \end{aligned} \quad (31)$$

Choosing the actuator torque as

$$\begin{aligned} \boldsymbol{\tau}_a^b &= -\mathbf{G}\mathbf{z}_1 - \mathbf{K}_2\mathbf{z}_2 + \boldsymbol{\omega}_{ib}^b \times (\mathbf{J}\boldsymbol{\omega}_{ib}^b) - \boldsymbol{\tau}_g^b \\ &\quad + \mathbf{J}\dot{\boldsymbol{\omega}}_{id}^b + \mathbf{J}\dot{\boldsymbol{\alpha}}_1 \end{aligned} \quad (32)$$

where $\mathbf{K}_2 = \mathbf{K}_2^T > 0$ is the feedback gain matrix for the \mathbf{z}_2 -system, leaves the LFC as

$$\begin{aligned} \dot{V}_2 &= \dot{V}_1 + \mathbf{z}_2^T [-\mathbf{G}\mathbf{z}_1 - \mathbf{K}_2\mathbf{z}_2] \\ &= -\mathbf{z}_1^T \mathbf{G}^T \mathbf{K}_1 \mathbf{G}\mathbf{z}_1 - \mathbf{z}_2^T \mathbf{K}_2\mathbf{z}_2 \\ &= -W(\mathbf{z}_1, \mathbf{z}_2) \leq 0 \end{aligned} \quad (33)$$

and the closed-loop dynamics as

$$\dot{\mathbf{z}}_1 = -\frac{1}{2}\mathbf{G}^T \mathbf{K}_1 \mathbf{G}\mathbf{z}_1 + \frac{1}{2}\mathbf{G}^T \mathbf{z}_2 \quad (34)$$

$$\mathbf{J}\dot{\mathbf{z}}_2 = -\mathbf{K}_2\mathbf{z}_2 - \mathbf{G}\mathbf{z}_1 \quad (35)$$

3.2 Stability

The stability properties of the closed loop system given by (34)-(35) follows from (31) and (33). From (31) it is seen that $V_2(\mathbf{z}_1, \mathbf{z}_2) > 0$, $V_2(0) = 0$ and $V_2(\mathbf{z}_1, \mathbf{z}_2) \rightarrow \infty$ as $(\mathbf{z}_1, \mathbf{z}_2) \rightarrow \infty$. Similarly, by (8) and (26) it can be shown that $W(\mathbf{z}_1, \mathbf{z}_2) > 0$ and $W(0) = 0$, and hence positive definite. According to the LaSalle-Yoshizawa theorem (Krstić *et al.*, 1995), this establishes that the equilibrium point $\mathbf{z}_e = (\mathbf{z}_1, \mathbf{z}_2) = (\mathbf{0}, \mathbf{0})$ is uniformly globally asymptotically stable (UGAS), which implies that $\tilde{\boldsymbol{\epsilon}} \rightarrow \mathbf{0}$ and $\tilde{\eta} \rightarrow \pm 1$. Henceforth, (23) implies that $\mathbf{q}(t) \rightarrow \mathbf{q}_d(t)$ as $t \rightarrow \infty$. Also, (24) and (29) implies that $\tilde{\boldsymbol{\omega}}(t) \rightarrow \mathbf{0}$ as $t \rightarrow \infty$.

Remark 1. It should be noted that the equilibrium point $\mathbf{z}_1 = \mathbf{0}$ corresponds to the two quaternion values $\tilde{\mathbf{q}} = [\pm 1 \ 0 \ 0 \ 0]^T$.

Remark 2. The controller given by (32) is similar to the one found in (Wen and Kreutz-Delgado, 1991). However, this controller has the advantage that the feedback from the quaternion error, described by the first term in (32), can be seen as a feedback with a state dependent gain matrix $\mathbf{G}(\tilde{\mathbf{q}})$. The result is that

as the quaternion error increases, the feedback gain will do the same. In addition, the absolute value in (22) leaves both quaternion values $\tilde{\mathbf{q}} = [\pm 1 \ 0 \ 0 \ 0]^T$ asymptotically stable. This ensures that a minimal rotation towards the equilibrium point is used, and the performance of the controller is improved. This topic is analyzed in detail in (Kristiansen and Nicklasson, 2004).

3.3 Implementation

The control law given by (32) contains the expression $\dot{\boldsymbol{\alpha}}_1$ that involves time derivatives of the states, and this should be avoided when the control law is implemented. The time differentiation can be performed as

$$\dot{\boldsymbol{\alpha}}_1 = -\mathbf{K}_1 \left[\dot{\mathbf{G}}(\tilde{\mathbf{q}})\mathbf{z}_1 + \mathbf{G}(\tilde{\mathbf{q}})\dot{\mathbf{z}}_1 \right]$$

where $\dot{\mathbf{z}}_1$ can be found from (25). Similarly, $\dot{\mathbf{G}}(\tilde{\mathbf{q}})$ can be expressed as

$$\dot{\mathbf{G}}(\tilde{\mathbf{q}}) = \frac{\partial \mathbf{G}}{\partial \tilde{\eta}} \dot{\tilde{\eta}} + \frac{\partial \mathbf{G}}{\partial \tilde{\boldsymbol{\epsilon}}} \dot{\tilde{\boldsymbol{\epsilon}}} = \begin{bmatrix} \text{sgn}(\tilde{\eta}) \dot{\tilde{\boldsymbol{\epsilon}}}^T \\ \dot{\tilde{\eta}} \mathbf{I} + \mathbf{S}(\tilde{\boldsymbol{\epsilon}}) \end{bmatrix}^T$$

The expressions for $\dot{\tilde{\eta}}$ and $\dot{\tilde{\boldsymbol{\epsilon}}}$ can be found from (13) and (14), respectively.

4. SIMULATIONS

4.1 Numerical values

The numerical values for the satellite ESEO have been used. The moments of inertia for the satellite is given as $\mathbf{I} = \text{diag} \{ 4.350 \ 4.3370 \ 3.6640 \}$ kgm² and the orbit altitude is 250 km, corresponding to the perigee altitude of the planned elliptic orbit. The maximum torque from the reaction thrusters is set to 0.13 N, and from the reaction wheel 0.4 Nm. The wheel moment of inertia is $4 \cdot 10^{-5}$ kgm², and the maximum angular velocity is 5035 rpm.

4.2 Results

The simulation results of the satellite with the backstepping controller (32) are presented in the following. The satellite body frame starts in perigee with zero initial angles, i.e. $\boldsymbol{\Theta}_i = [0^\circ \ 0^\circ \ 0^\circ]^T$ and the desired angles are $\boldsymbol{\Theta}_d = [-75^\circ \ -175^\circ \ 70^\circ]^T$ relative to the orbit frame in perigee. This corresponds to the quaternion values $\mathbf{q}_i = [\pm 1 \ 0 \ 0 \ 0]^T$ and $\mathbf{q}_d = [-0.3772 \ -0.4329 \ 0.6645 \ 0.4783]^T$. The satellite is further commanded to follow a trajectory that rotates the body frame one evolution about the orbit frame every orbit cycle. This corresponds to keeping the attitude constant relative to the ECI frame. Fig. 1 shows the satellite settling to the desired attitude, and Fig. 2 shows attitude tracking over approximately two orbits. The satellite is shown to settle within approximately 38 seconds, and manages to maintain the desired attitude constant over the entire orbit.

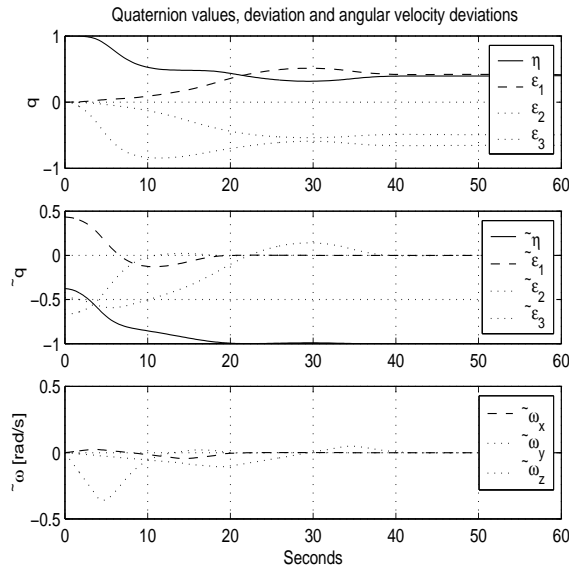


Fig. 1. Satellite settling at desired values. The plot shows quaternion values \mathbf{q} , quaternion deviation $\tilde{\mathbf{q}}$ and angular velocity deviation $\tilde{\boldsymbol{\omega}}$

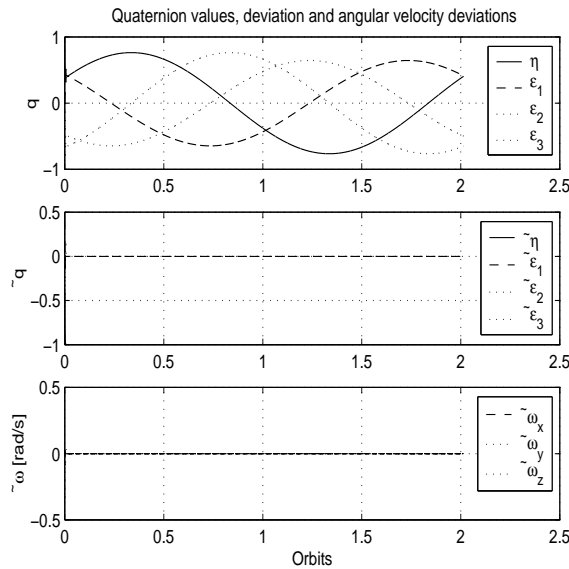


Fig. 2. Satellite tracking the desired attitude. The plot shows quaternion values \mathbf{q} , quaternion deviation $\tilde{\mathbf{q}}$ and angular velocity deviation $\tilde{\boldsymbol{\omega}}$

5. CONCLUSION

In this paper we have presented a quaternion feedback controller based on a quaternion product and integrator backstepping, that asymptotically tracks a smooth attitude reference. This has been proved by the use of the LaSalle-Yoshizawa theorem. Simulations of the ESEO satellite incorporating four thrusters and one reaction wheel have also been presented to illustrate that the controller gives acceptable performance. The thrusters are controlled by a bang-bang deadzone algorithm. Future work will emphasize the extension of this controller to the case of system parameter adaptation. Also, analysis of stability when PWM/PWPFM is utilized for thruster control should be investigated.

REFERENCES

- Akella, M. R. (2001). Rigid body attitude tracking without angular velocity feedback. *System & Control Letters* **42**, 321–326.
- Antonsen, J. (2004). Attitude control of a microsatellite with the use of reaction control thrusters. Master's thesis. Narvik University College. Narvik, Norway.
- Caccavale, F. and L. Villani (1999). Output feedback control for attitude tracking. *System & Control Letters* **38**, 91–98.
- Egeland, O. and J. T. Gravdahl (2002). *Modeling and Simulation for Automatic Control*. Marine Cybernetics. Trondheim, Norway.
- Fjellstad, O.-E. (1994). Control of Unmanned Underwater Vehicles in Six Degrees of Freedom. PhD thesis. Department of Engineering Cybernetics, Norwegian University of Science and Technology. Trondheim, Norway.
- Fossen, T. I. (2002). *Marine Control Systems*. Marine Cybernetics. Trondheim, Norway.
- Jensen, H. B. and R. Wisniewski (2001). Quaternion feedback control for rigid-body spacecraft. In: *Proceedings of the AIAA Guidance, Navigation and Control Conference*. Montreal, Canada.
- Joshi, S. M., A. G. Kelkar and J. T.-Y. Wen (1995). Robust attitude stabilization of spacecraft using nonlinear quaternion feedback. *IEEE Transactions on Automatic Control* **40**(10), 1800–1803.
- Kristiansen, R. and P. J. Nicklasson (2004). Satellite attitude control by quaternion-based backstepping. Internal report, Narvik University College.
- Krstić, M., I. Kanellakopoulos and P. Kokotović (1995). *Nonlinear and Adaptive Control Design*. John Wiley & Sons, Inc. New York.
- Romano, M. and B. N. Agrawal (2003). Acquisition, tracking and pointing control of the bifocal relay mirror spacecraft. *Acta Astronautica* **53**, 509–519.
- Sidi, M. J. (1997). *Spacecraft Dynamics and Control*. Cambridge University Press. New York.
- Song, G. and B. N. Agrawal (2001). Vibration suppression during attitude control. *Acta Astronautica* **49**(2), 73–83.
- Strang, G. (1988). *Linear Algebra and its Applications*. Harcourt Brace Jovanovich College Publishers. Orlando, Florida, USA.
- Topland, M. and J. T. Gravdahl (2004). Nonlinear attitude control of the microsatellite ESEO. In: *Proceedings of The 55th International Astronautical Congress*. Vancouver, Canada.
- Wang, P., Y. B. Shtessel and Y. Wang (1998). Satellite attitude control using only magnetorquers. In: *Proceedings of the Thirtieth Southeastern Symposium on System Theory*.
- Wen, J. T.-Y. and K. Kreutz-Delgado (1991). The attitude control problem. *IEEE Transactions on Automatic Control* **36**(10), 1148–1162.